Nuclear hormone receptor corepressor promotes esophageal cancer cell invasion by transcriptional repression of interferon-γ–inducible protein 10 in a casein kinase 2–dependent manner

Jung-Yoon Yoo[a,*], Hyo-Kyoung Choi[a,*], Kyung-Chul Choi[b], Soo-Yeon Park[a], Ichiro Ota[c], Jong In Yook[d], Yoo-Hyun Lee[e], Kunhong Kim[a], and Ho-Geun Yoon[a]

[a]Department of Biochemistry and Molecular Biology, Brain Korea 21 Project for Medical Sciences, Severance Medical Research Institute, Yonsei University College of Medicine, Seoul 120-752, Korea; [b]Department of Medicine, Graduate School, University of Ulsan, Seoul 138-736, Korea; [c]Department of Otolaryngology, Nara Medical University, Nara 634-8521, Japan; [d]Department of Oral Pathology, Yonsei University College of Dentistry, Seoul 120-752, Korea; [e]Department of Food and Nutrition, University of Suwon, Suwon 445-743, South Korea

ABSTRACT **Aberrant expression of casein kinase 2 (CK2) is associated with tumor progression; however, the molecular mechanism by which CK2 modulates tumorigenesis is incompletely understood. In this paper, we show that CK2α phosphorylates the C-terminal domain of the nuclear receptor corepressor (NCoR) at Ser-2436 to stabilize the NCoR against the ubiquitin-dependent proteasomal degradation pathway. Importantly, NCoR promoted the invasion of esophageal cancer cells in a CK2-dependent manner. By using cyclic DNA microarray analysis, we identified CXCL10/IP-10 as a novel CK2α-NCoR cascade–regulated gene. The depletion of both NCoR and HDAC3 commonly derepressed IP-10 transcription, demonstrating the functional engagement of the NCoR-HDAC3 axis in IP-10 transcriptional repression. Furthermore, chromatin immunoprecipitation assays showed that c-Jun recruits NCoR-HDAC3 corepressor complexes to the (AP1 site of IP-10, leading to histone hypoacetylation and IP-10 down-regulation. Collectively these data suggest that the CK2α-NCoR cascade selectively represses the transcription of IP-10 and promotes oncogenic signaling in human esophageal cancer cells.**

Monitoring Editor
Kunxin Luo
University of California, Berkeley

Received: Nov 28, 2011
Revised: May 24, 2012
Accepted: May 31, 2012

This article was published online ahead of print in MBoC in Press (http://www.molbiolcell.org/cgi/doi/10.1091/mbc.E11-11-0947) on June 6, 2012.

*These authors contributed equally to this work.

The authors declare no conflict of interest.

Address correspondence to: Ho-Geun Yoon (yhgeun@yuhs.ac).

Abbreviations used: AP1, activator protein 1; CAM, chorioallantoic membrane; cDNA, cyclic DNA; ChIP, chromatin immunoprecipitation; CK2, casein kinase 2; DMSO, dimethyl sulfoxide; EMT, epithelial–mesenchymal transition; F, forward primer sequence; FBS, fetal bovine serum; GFP, green fluorescent protein; GPS2, G-protein pathway suppressor 2; GST, glutathione *S*-transferase; HA, hemagglutinin; HDAC3, histone deacetylase 3; IgG, immunoglobulin G; IP-10, interferon-γ–inducible protein 10; NCoR, nuclear hormone receptor corepressor; NR, nuclear receptor; NRID, nuclear hormone receptor interacting domain; PLA, proximity ligation assay; R, reverse primer sequence; siRNA, small interfering RNA; SMRT, silencing mediator for retinoic and thyroid receptors; TBB, 4,5,6,7-tetrabromo-2-azabenzimidazole; TBL1, transducin-β–like protein 1; TBLR1, TBL1 receptor; TR, thyroid hormone receptor; Ubc9, ubiquitin-conjugating enzyme 9.

INTRODUCTION

The nuclear receptor corepressor (NCoR) and silencing mediator for retinoic and thyroid receptors (SMRT) are well-known corepressors of nuclear receptors (NRs) and many other transcription factors (Perissi *et al*., 2010). Both NCoR and SMRT form corepressor complexes with histone deacetylase 3 (HDAC3) that induce changes in local chromatin structure, causing transcriptional repression. The N-terminus of NCoR contains four repression domains associated with protein–protein interactions that mediate the formation of a core complex with transducin-β–like protein 1 (TBL1), the TBL1 receptor 1 (TBLR1), G-protein pathway suppressor 2 (GPS2), and HDAC3 (Yoon *et al*., 2003a,b). The receptor interaction domain resides in the C-terminal half of NCoR and recognizes and binds to unliganded NRs (Seol *et al*., 1996). Accumulated studies have shown that the function of NCoR and SMRT in transcriptional repression is regulated by posttranslational modification. The sumoylation of NCoR by SUMO and ubiquitin-conjugating enzyme 9 (Ubc9), an E2 conjugation enzyme, results in enhanced NCoR-dependent transcriptional

Supplemental Material can be found at:
http://www.molbiolcell.org/content/suppl/2012/06/04/mbc.E11-11-0947.DC1.html

repression (Tiefenbach *et al.*, 2006). IKKα kinase has been shown to be recruited to chromatin in response to various stimuli; once localized, it phosphorylates SMRT at Ser-2410. SMRT phosphorylation leads to nuclear export and proteasomal degradation, reducing repression (Hoberg *et al.*, 2004). In addition to IKKα, casein kinase 2 (CK2) phosphorylates SMRT on Ser-1492, which stabilizes the association between SMRT and thyroid hormone receptors, thus enhancing repression (Zhou *et al.*, 2001). Importantly, although the C-terminal domain of NCoR also possesses the same CK2 phosphorylation site as SMRT, the effect of CK2-mediated NCoR phosphorylation on its function has not been explored.

CK2 is a multifunctional protein kinase with over 300 substrates, many of which are critically involved in cell cycle control, cellular differentiation, proliferation, and metabolic pathways (Ruzzene and Pinna, 2010). Additionally, CK2 dysregulation in tumor cells may influence apoptotic activity and enhance cell survival (Guo *et al.*, 2001). Furthermore, CK2 expression levels and activities are known to be increased three- to fivefold in many tumors and tumor cell lines (Trembley *et al.*, 2009). In transgenic mice, CK2 overexpression cooperates with c-myc or loss (or mutation) of p53 at the lpr locus to promote tumorigenesis (Landesman-Bollag *et al.*, 2001). CK2 plays a positive role in Wnt/β-catenin signaling via β-catenin phosphorylation at Thr-393, leading to proteasomal resistance and increased cotranscriptional activity (Song *et al.*, 2003). Importantly, CK2 participates in the control of Snail1, a major factor for the epithelial–mesenchymal transition (EMT), by stabilizing and positively regulating the repressive function of Snail1 and its interaction with the corepressor mSin3A (MacPherson *et al.*, 2010). CK2 also phosphorylates osteopontin, a protein that correlates with tumor invasion, progression, or metastasis in multiple cancers, including cancers of the breast, stomach, lung, prostate, liver, and colon (Christensen *et al.*, 2005; Trembley *et al.*, 2009; Giusiano *et al.*, 2010). Additionally, emodin, a selective inhibitor of CK2 activity, significantly inhibits invasion of human tongue cancer SCC-4 cells by MMP-9 down-regulation (Chen *et al.*, 2010). Although aberrant expression of CK2 is known to be involved in many cancers, the mechanism by which CK2 promotes tumorigenesis remains obscure.

In this study, we found that CK2α directly bound and phosphorylated the C-terminal domain of NCoR. We show that CK2α-mediated phosphorylation stabilized NCoR against ubiquitin-dependent proteasomal degradation. We also show that CK2α-dependent NCoR phosphorylation is required for transcriptional repression of interferon-γ–inducible protein 10 (IP-10) and invasion of esophageal cancer cells. This study unravels the unique role of the CK2α-NCoR oncogenic cascade in human esophageal cancer cells.

RESULTS

CK2α specifically interacts with the nuclear hormone receptor interacting domain (NRID) of NCoR and phosphorylates the C-terminal NRID domain

To elucidate the functional role of the NCoR protein in cellular signaling, we first attempted to identify NCoR-interacting proteins using yeast two-hybrid screening. Human HeLa and testis cyclic DNA (cDNA) libraries were screened using multiple NCoR domains. Based on sequence analysis, CK2α was selected as a putative NCoR-interacting protein (unpublished data). To confirm the yeast two-hybrid assay results, we performed in vitro and in vivo pulldown assays. Immunoprecipitation analysis revealed that Myc-tagged CK2α specifically interacted with endogenous NCoR protein. Consistently, reciprocal immunoprecipitation analysis verified the endogenous interaction between NCoR and CK2α (Figure 1A). Mapping analysis using GST pulldown and immunoprecipitation assays showed that the NRID of NCoR directly interacted with CK2α, but not with CK2β (Figure 1B and Supplemental Figure S1, A and B). Thus a specific interaction domain of NCoR with CK2α was mapped to the region between residues 1985 and 2440 in NCoR (NCoR-15/16 [NRID]).

We next examined whether CK2α directly phosphorylates the NCoR-15/16 domain by performing in vitro kinase assays using various GST-NCoR-15/16 domain proteins as indicated in Figure 1C. CK2α efficiently phosphorylated the C-terminal region of the NCoR-15/16-3 domain (Figures 1C and S1C), suggesting that the target phosphorylation site of CK2α may be located within the NCoR-15/16-3 domain. To verify the in vitro kinase assay results, we assessed inhibition of NCoR phosphorylation using a specific inhibitor against CK2—4,5,6,7-tetrabromo-2-azabenzimidazole (TBB). As expected, TBB dose-dependently blocked CK2α-dependent NCoR phosphorylation in vitro (Figure S1D). To confirm CK2α-dependent NCoR phosphorylation in vivo, we transfected HeLa cells with the FLAG-tagged NCoR-15/16 expression plasmid with CK2α expression plasmids with or without TBB. The phosphoform of NCoR-15/16 was detected by coexpression of CK2α; however, 50 μM of TBB completely blocked NCoR-15/16 phosphorylation with negligible effect on the cytotoxicity (unpublished data), indicating that NCoR is phosphorylated by CK2α in vivo (Figure S1E).

CK2a phosphorylates the Ser-2436 residue of NCoR

To identify the critical amino acid for CK2α-dependent NCoR phosphorylation, we used the computational NetPhosK 1.0 prediction program. Sequence analysis predicted three phosphorylation sites in the NRID domain (Figure S2A). For accurate determination of the phosphorylation site in NCoR, we generated glutathione *S*-transferase (GST)-tagged mutant plasmids in which serine was substituted for alanine, and mutant plasmids were screened using in vitro kinase assays. Replacement with alanine of both Ser-2143 and Ser-2144 in the NRID domain had a negligible effect on phosphorylation; however, mutation of Ser-2436 resulted in complete loss of phosphorylation in the NRID domain, providing evidence that the Ser-2436 residue of NCoR is critical for CK2α-dependent phosphorylation (Figure 1D).

To further examine whether NCoR Ser-2436 is phosphorylated by CK2α and to study the biological importance of phosphorylation at this site, we generated a phosphospecific NCoR antibody that specifically recognizes phosphorylated Ser-2436 (Ser(P)-2436) in NCoR. Polyclonal antibodies were generated against the NCoR phosphopeptide ^{2431}CQYETL*p*SDSDD^{2440} (Figure S2B), and the antisera were tested by Western blot analysis after in vitro kinase reaction. Specificity of the antibodies was shown by recognition that NCoR-15/16^{WT}, but not NCoR-15/16^{S2436A}, could be phosphorylated at this site (Figure 1E). Furthermore, a peptide competition assay clearly exhibited the specificity of the NCoR Ser(P)-2436 antibody through complete blocking of NCoR phosphorylation by treatment of the phosphopeptide but not by a nonphosphopeptide (Figure S2C). To further test the specificity of the antibody, we cotransfected HeLa cells with green fluorescent protein (GFP)-tagged variants of wild-type NCoR, NCoR$^{S2143/2144A}$, NCoR^{S2436A}, and/or Myc-tagged CK2α. Cell lysates were immunoprecipitated with GFP antibody and subjected to Western blot analysis using the NCoR Ser(P)-2436 antibody. The phosphospecific antibody detected Ser-2463 in NCoR^{WT} and the NCoR$^{S2143/2144A}$ double mutant, but not in the NCoR^{S2436A} mutant. As a control, TBB treatment completely blocked recognition of NCoR^{WT} by the NCoR Ser(P)-2436 antibody, confirming the specificity of the phosphospecific antibody (Figure 1F). Notably, TBB treatment greatly reduced both NCoR

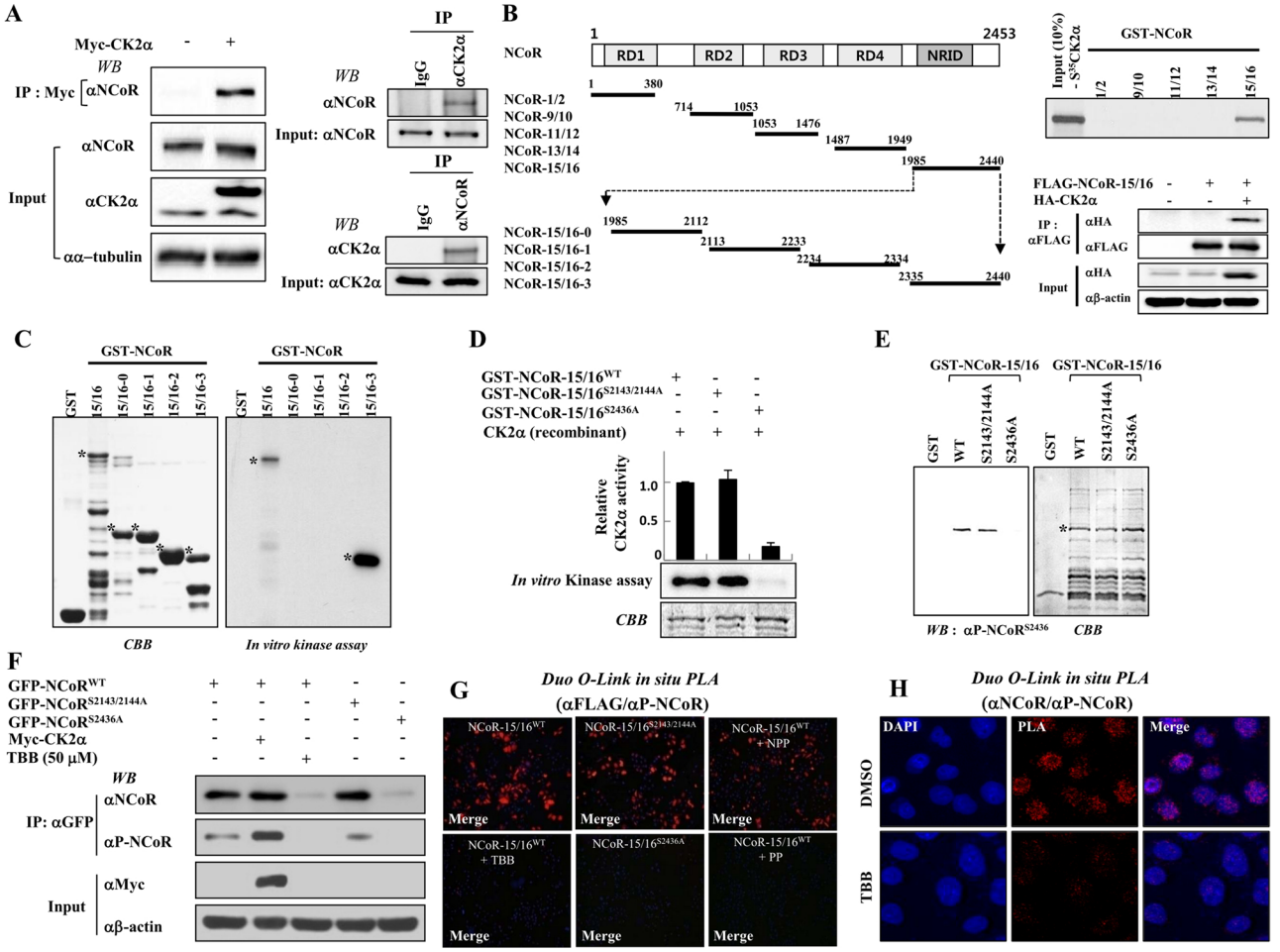

FIGURE 1: CK2α phosphorylates Ser-2436 of NCoR. (A) Reciprocal immunoprecipitation analysis was performed using HeLa cell lysates with a CK2α or NCoR antibody, and immunoblotting was performed using their respective antibodies (right). HeLa cells were transfected with Myc-CK2α, and cell lysates were immunoprecipitated and immunoblotted with their respective antibodies (left). (B) A schematic of the deletion mutants of NCoR for in vitro translation (left). Bound proteins were eluted and analyzed by autoradiography (right, top). HeLa cells were transfected with FLAG-tagged NCoR-15/16 (1985–2440) and HA-tagged CK2α plasmids. Whole-cell lysates were immunoprecipitated and immunoblotted with the indicated antibodies (right, bottom). (C and D) In vitro kinase assays were performed with CK2α and the indicated GST-fused NCoR-15/16 proteins. Bound proteins were eluted and analyzed by autoradiography (C) and scintillation counter (D). (E) In vitro kinase assays were performed with recombinant CK2α enzyme and the indicated GST-fused NCoR-15/16 proteins. Western blotting was performed with phospho-NCoR antibody. *CBB*, Coomassie blue staining. (F) Full-length GFP-NCoR plasmids were transfected into HeLa cells with or without Myc-CK2α and treated with TBB (50 μM) for 6 h. Cell lysates were analyzed by Western blotting with indicated antibodies. (G) HeLa cells were seeded on coverslips and transfected with the indicated expression plasmids in the presence or absence of TBB (50 μM). The permeabilized HeLa cells were incubated with indicated antibodies and/or 1 μg/ml of non-phosphopeptide (NPP) or phosphopeptide (PP) for 12 h, which was followed by PLA probes (PLUS and MINUS) treatment. The positive signal was analyzed using confocal microscopy. (H) In situ PLA analysis was performed under the same conditions as above without transfection of expression plasmids. The level of NCoR phosphorylation was assessed with αNCoR antibody and α-phospho-NCoR antibody.

and NCoR phosphorylation levels, implying a functional role of CK2α-mediated phosphorylation in NCoR stability.

To verify the in vivo NCoR phosphorylation by CK2α, we performed a proximity ligation assay (PLA) using the Duolink in situ PLA kit (Soderberg *et al.*, 2006). NCoR-15/16^{WT} protein was efficiently phosphorylated in HeLa cells (Figure 1G), whereas TBB treatment in the same cells resulted in loss of phosphorylation events similar to that seen with the control plasmid (Figure S2D). Consistently, FLAG-tagged NCoR-15/16$^{S2143/2144A}$ showed similar patterns of phosphorylation compared with NCoR-15/16^{WT}; however, mutant FLAG-tagged NCoR-15/16^{S2436A} displayed no phosphorylation events similar to those of control (Figure S2E). Importantly, the phosphopeptide, but not the nonphosphopeptide, completely blocked phosphorylation of NCoR. More importantly, TBB treatment completely abrogated endogenous NCoR phosphorylation by PLA analysis (Figure 1H). These data clearly indicated CK2α-dependent NCoR phosphorylation in vivo. Finally, to confirm that the modification by CK2 occurs at Ser-2436, the nonphosphopeptide corresponding region between residues 2431 and 2440 of NCoR was incubated with immunoprecipitated CK2 and/or TBB and subjected to matrix-assisted laser desorption ionization time-of-flight analysis. A peptide with molecular mass corresponding to the Ser-2436–phosphorylated peptide

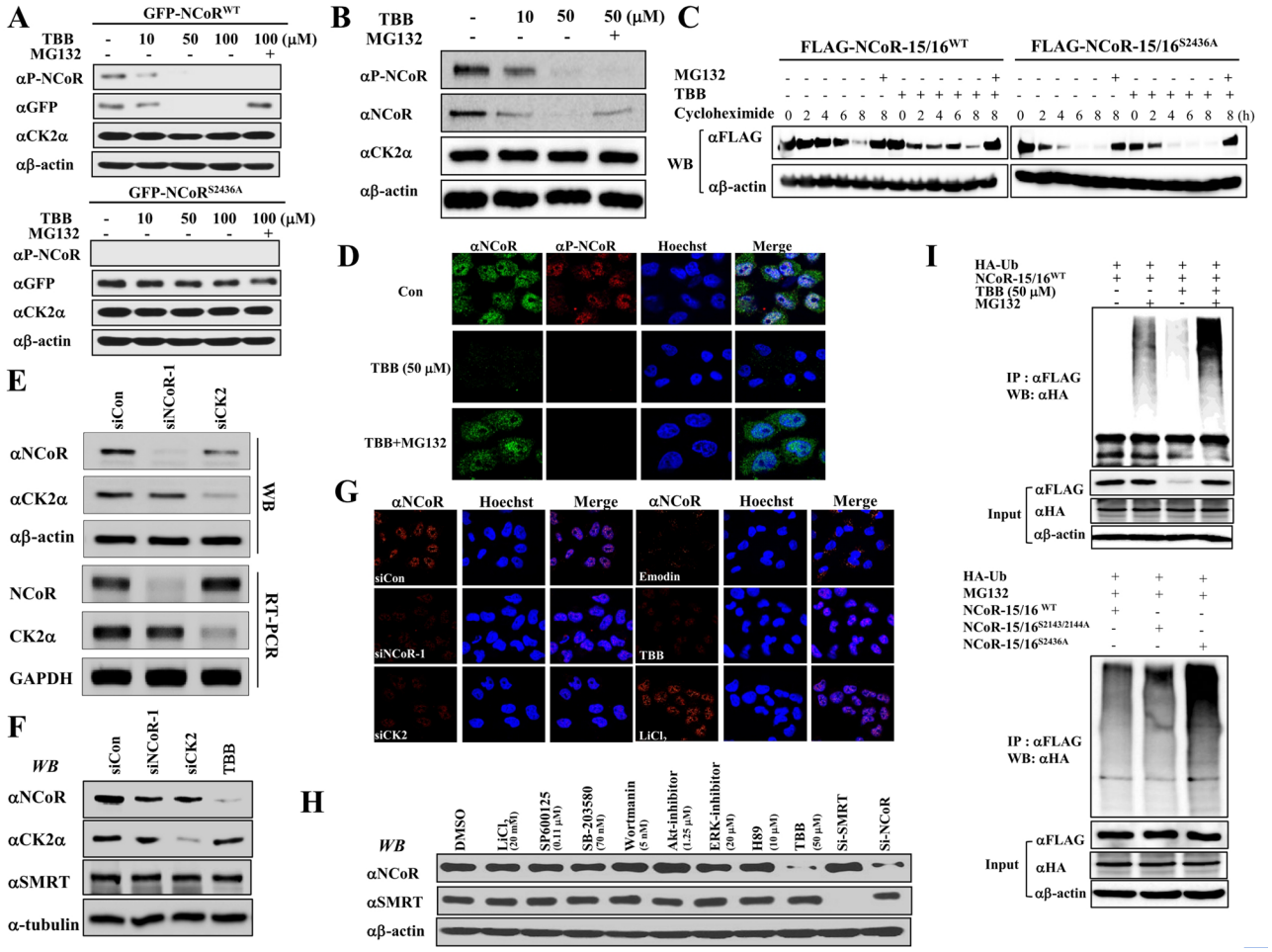

FIGURE 2: CK2α-dependent NCoR phosphorylation increases NCoR stability via inhibition of the ubiquitin-dependent proteasomal pathway. (A) HeLa cells were transfected with full-length GFP-NCoR plasmids and treated with an increase amount of TBB (10, 50, 100 μM) and/or MG132 (10 μM) for 6 h. Cell lysates were analyzed by Western blotting. (B) HeLa cells were treated with an increase amount of TBB (10, 50 μM) and/or MG132, and cell lysates were analyzed by Western blotting with indicated antibodies. (C) HeLa cells were transfected with either FLAG-NCoR-15/16^{WT} or FLAG-NCoR-15/16^{S2436A} plasmid. After 2 d, cells were treated with cycloheximide (10 μg/ml), TBB (50 μM), and/or MG132 for various time periods, and cell lysates were analyzed by Western blotting. (D) HeLa cells were treated with TBB (50 μM) and/or MG132, and endogenous NCoR and phospho-NCoR levels were analyzed by confocal microscopy. (E and F) HeLa cells were treated with TBB (50 μM) or siRNAs against NCoR or CK2α, and then protein and mRNA levels were analyzed by Western blotting (E) and RT-PCR (F), respectively. (G) HeLa cells were treated with emodin (50 μM), TBB, $LiCl_2$, and indicated siRNAs, and endogenous NCoR levels were then analyzed by confocal microscopy. (H) HeLa cells were treated with indicated inhibitors or siRNAs, and cell lysates were analyzed by Western blotting. (I) FLAG-NCoR-15/16 plasmids and HA-ubiquitin (Ub) were transfected into HeLa cells with TBB and/or MG132, and cell lysates were analyzed by Western blotting.

was observed after addition of CK2, whereas TBB treatment failed to show the peak corresponding to the phosphorylated peptide (Figure S3). Together these data establish that Ser-2436 is a major NCoR phosphorylation site in vivo and can be activated by CK2.

CK2 stabilizes NCoR via inhibition of the ubiquitin-dependent proteasomal degradation pathway

To elucidate the effect of CK2-mediated phosphorylation on the function of NCoR, we first examined whether CK2-dependent phosphorylation affected the stability of the NCoR protein. TBB treatment dose-dependently decreased both expression and phosphorylation of full-length NCoR^{WT}; however, TBB had a negligible effect on NCoR^{S2436A} (Figure 2A). Interestingly, MG132 treatment restored the TBB-induced decrease in the level of NCoR^{WT} relative to NCoR^{S2436A}. To confirm this result, we examined the level of phosphorylation and stability of endogenous NCoR. As expected, TBB treatment dramatically reduced NCoR phosphorylation and stability, whereas MG132 treatment reversed NCoR stability (Figure 2B). Additionally, a time-course experiment with cycloheximide treatment again verified that CK2-dependent phosphorylation maintains NCoR stability (Figures 2C and S4A). Interestingly, the subcellular localization of dephosphorylated NCoR was similar to that seen in the control, indicating that CK2-dependent phosphorylation had no effect on the cellular distribution of NCoR (Figure 2D).

We next sought to examine the knockdown effect of CK2 on NCoR stability. We designed small interfering RNAs (siRNAs) against CK2 and NCoR. After establishing the specific knockdown efficiency of each siRNA by Western blot analysis (Figure 2E), we performed immunostaining analysis in HeLa cells after treatment with siNCoR, siCK2, TBB, or another specific inhibitor against CK2, Emodin. Both

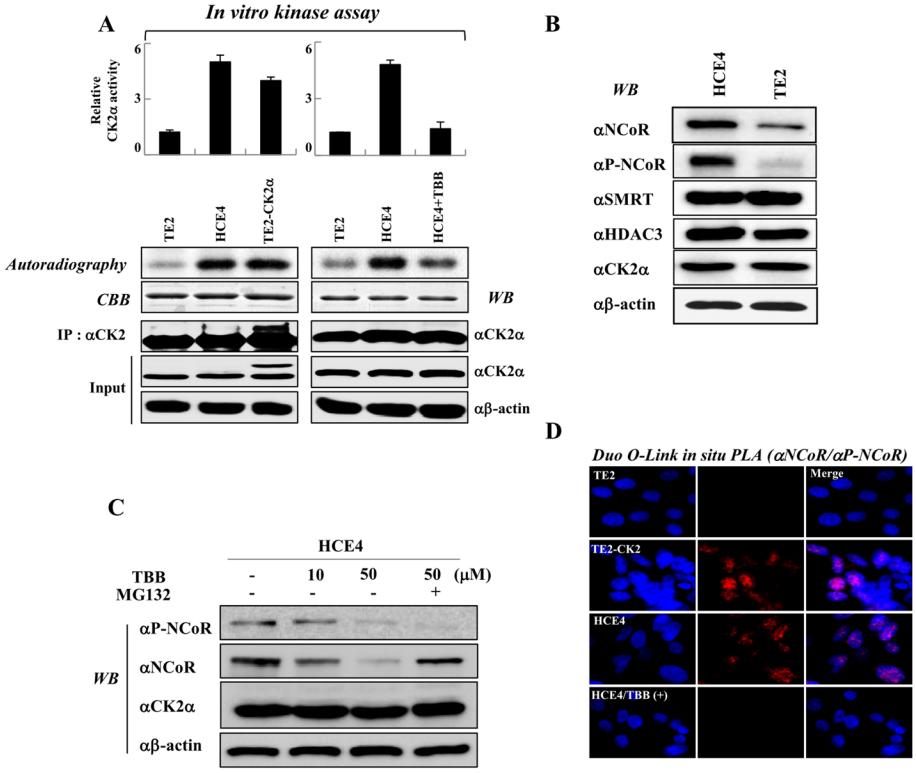

FIGURE 3: The levels of NCoR phosphorylation at Ser-2436 are well associated with patterns of CK2α activities. (A) In vitro kinase assays were performed by incubation of GST-NCoR-15/16 protein and immunoprecipitated CK2α enzyme from TE2, TE2-CK2α and HCE4 cells, and CK2α phosphorylation levels were analyzed by autoradiography and scintillation counter. (B) Whole-cell lysates from TE2 and HCE4 cells were analyzed by Western blotting. (C) HCE4 cells were treated with TBB (10, 50 μM) and/or MG132 for 6 h, and cell lysates were analyzed by Western blotting. (D) TE2, TE2-CK2α, and HCE4 cells were seeded on coverslips and treated with or without TBB (50 μM). Permeabilized cells were incubated with a phosphospecific NCoR antibody, an NCoR antibody, and PLA probes. Duolink in situ PLA analysis was performed as described in *Materials and Methods*.

knockdown of CK2 and inhibition of CK2 activity dramatically reduced the endogenous NCoR level, likely silencing NCoR (Figures 2G and S4B). Consistently, MG132 treatment dramatically restored the level of endogenous NCoR (Figure 2D) without affecting the level of NCoR phosphorylation. Notably, CK2 knockdown led to reduced NCoR protein levels, but not reduced NCoR mRNA levels, further supporting our notion that CK2 plays an important role in NCoR stability (Figure 2E). Because SMRT is known to be phosphorylated by CK2, we examined whether CK2-dependent phosphorylation is also required for SMRT stability. Either depletion of CK2 or TBB treatment had no effect on SMRT levels, suggesting the differential effect of CK2-dependent phosphorylation on both proteins (Figure 2, F and H). Notably, NCoR stability was specifically abolished by only TBB and not by other kinase-specific inhibitors (Figure 2H). Because a previous study showed NCoR is degraded following overexpression of Siah1 (Perissi *et al.*, 2004), we investigated whether CK2-mediated phosphorylation of NCoR suppresses the Siah1-mediated degradation of NCoR. Consistent with previous findings, overexpression of Siah1 reduced the stability of endogenous NCoR, whereas overexpressed CK2 efficiently blocked the Siah1-mediated degradation of NCoR. As expected, TBB treatment again reduced the stability of NCoR, indicating that phosphorylation of NCoR by CK2 antagonizes the Siah1-mediated NCoR degradation (Figure S5).

As MG132 treatment blocked TBB-induced degradation of NCoR, we investigated whether inhibition of NCoR phosphorylation by TBB induced the ubiquitination of NCoR. TBB treatment increased the ubiquitination of the NCoR-15/16^{WT} domain and MG132 treatment further enhanced the effect by TBB (Figure 2I). Furthermore, ubiquitination of NCoR-15/16^{S2436A} was greatly increased by MG132 compared with both NCoR-15/16^{WT} and NCoR-15/16$^{S2143/2144A}$. Collectively these data indicate that CK2-dependent phosphorylation is critical for NCoR stability via the ubiquitin-dependent proteasomal degradation pathway.

NCoR promotes the invasion of cancer cells in a CK2-dependent manner

Two esophageal cancer cell lines, TE2 and HCE4, display opposing levels of CK2 activities with a similar level of CK2 itself (Shin *et al.*, 2005). We therefore examined the biological importance of CK2-mediated NCoR phosphorylation using these cells as a model system. To confirm the previous report, we first assessed the relative activity of CK2 in both lines. In vitro kinase assays revealed that CK2 activities in both HCE4 and TE2-CK2 cells that stably express CK2 are fivefold higher than in TE2 cells (Figures 3A and S6); however, TBB treatment of HCE4 cells decreased CK2 activity. Importantly, the patterns of NCoR expression and phosphorylation were well associated with those of CK2 activity (Figure 3B). Consistently, TBB treatment greatly reduced both phosphorylation and stability of NCoR in HCE4 cells, whereas MG132 treatment restored the reduced NCoR level induced by TBB treatment (Figure 3C). To confirm these results, we performed in situ PLA analysis to compare endogenous levels of NCoR and phospho-NCoR in both cancer cell lines. Consistent with the Western blot analysis, positive signals from HCE4 cells were higher than those from TE2 cells, and TBB treatment decreased the phospho-NCoR level in HCE4 cells, confirming that NCoR phosphorylation levels are well associated with patterns of CK2 activities in both cancer cell lines (Figure 3D).

Because multiple clinical observations have implicated CK2 in tumorigenesis of cancer cells (Trembley *et al.*, 2009), we investigated whether NCoR is required for CK2-mediated invasion of esophageal cancer cells. The invasiveness of HCE4 and CK2-overexpressing TE2 cells were sevenfold higher than that of TE2 cells (Figure 4A). The patterns of invasion activity in both cancer cell lines are closely correlated with CK2 activity, as either TBB treatment or knockdown of CK2 efficiently reversed the invasiveness of both cell types (Figure 4B). Interestingly, combinatorial treatment with siRNAs against NCoR and TBB synergistically suppressed the invasiveness of HCE4 cancer cells as compared with individual treatment (Figures 4C, S7, and S8A). More interestingly, overexpression of mutant NCoR^{S2436A} protein failed to enhance the invasiveness of HCE4 cells compared with wild-type NCoR, suggesting that CK2-mediated phosphorylation of NCoR is crucial for NCoR-mediated invasion of cancer cells. These data collectively demonstrate a crucial role of

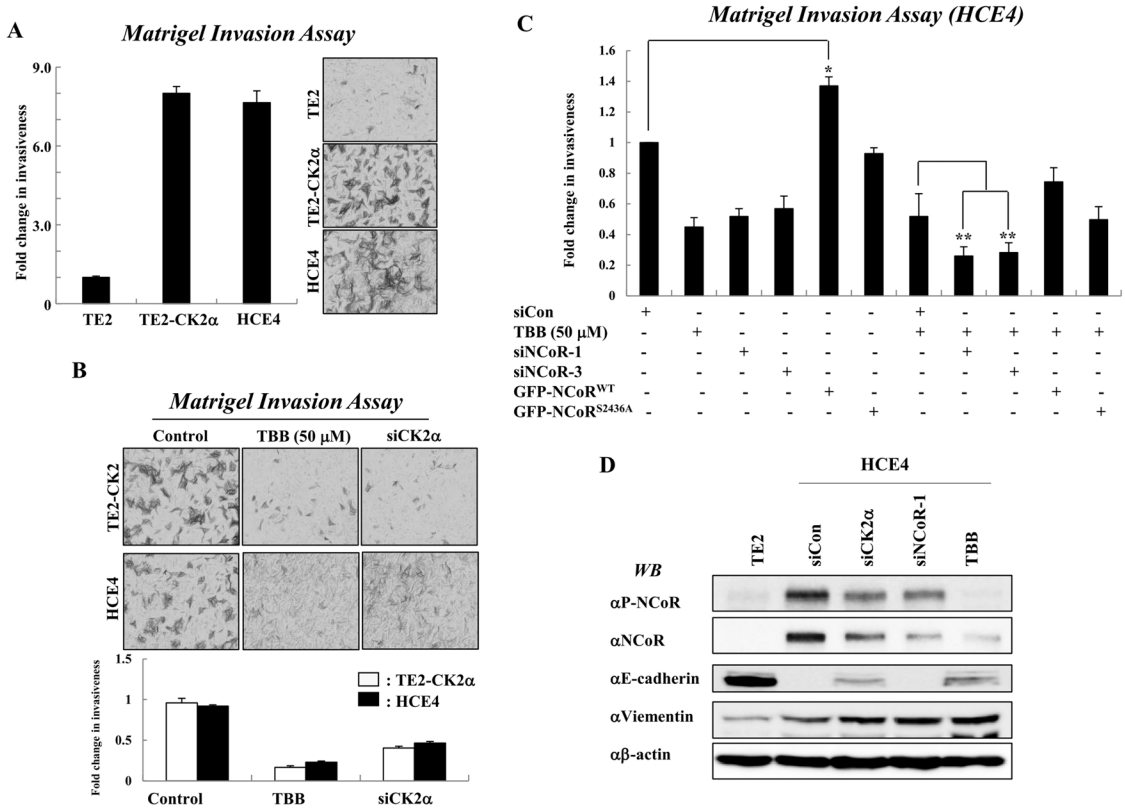

FIGURE 4: NCoR promotes the invasion of esophageal cancer cells in a CK2α-dependent manner. (A) Invasion was analyzed by counting cells that migrated through the extracellular matrix layer of BioCoat Matrigel invasion chambers. Data are expressed as the means ± SD of at least three independent experiments. (B) Both TE2-CK2α and HCE4 cells were transfected with siRNAs against NCoR and/or TBB (50 μM) before application to the upper chamber. Data are expressed as the means ± SD of at least three independent experiments. (C) HCE4 cells were treated with individual siNCoRs, GFP-NCoR plasmids, and/or TBB, and invasion was analyzed by counting cells that migrated through the extracellular matrix layer of BioCoat Matrigel invasion chambers. *, $p < 0.05$ vs. siCon; **, $p < 0.01$ vs. siCon + TBB. (D) Either TE2 or HCE4 cell was treated with indicated siRNAs or TBB, and cell lysates were analyzed by Western blotting.

NCoR in CK2-mediated invasion of cancer cells. Importantly, CK2 is known to phosphorylate E-cadherin and the positive regulator Snail1, a major factor for EMT. Thus we examined whether the CK2-NCoR network is also required for down-regulation of E-cadherin. E-cadherin levels were greatly decreased in HCE4 cells and derepressed with TBB or siCK2 treatment (Figure 4D). This reversed pattern of E-cadherin expression likely depends on the level of CK2, but not of NCoR, because silencing of NCoR had a negligible effect on the levels of E-cadherin. Furthermore, the depletion of both CK2 and NCoR had no effect on the elevated level of another tumor metastasis marker protein, vimentin. These data suggest that NCoR plays a role in CK2-dependent invasion of tumor cells via an alternative pathway.

CK2-NCoR cascade represses the transcription of the anti-tumorigenic gene IP-10 to promote the invasion of esophageal cancer cell

Given the significant role of CK2-induced NCoR phosphorylation in the invasion of cancer cells, we sought to unravel how NCoR modulates the tumorigenicity of cancer cells in a CK2-dependent manner. Because NCoR is a well-known transcriptional corepressor for diverse transcription factors via suppression of specific target genes (Perissi *et al.*, 2010), we screened tumorigenesis-related genes regulated by the CK2-NCoR cascade. cDNA microarray analysis revealed that 64 and 9 genes were derepressed by siCK2 and siNCoR treatment, respectively (Figures 5A and S8B). Among genes derepressed by depletion of either CK2 or NCoR, those coderepressed by more than twofold were selected. Four genes were identified: *topomyosin 4* (*TPM4*), *opioid growth factor receptor* (*OGFR*), *interferon-induced protein with tetratricopeptide repeats 1* (*IFIT1*), and *IP-10*. Both reverse transcriptase (RT)-PCR and real-time PCR analysis validated the cDNA microarray analysis results, confirming the derepression of the four genes by knockdown of either CK2 or NCoR and the differential expression of the four genes in both TE2 and HCE4 cells (Figures 5B and S8C). These results revealed that the four genes are novel CK2-NCoR cascade–regulated genes.

Among them, *IP-10* (*CXCL10*) promotes cell-mediated immunity and inhibits proliferation and metastasis in many tumors (Tominaga *et al.*, 2007; Mei *et al.*, 2008; Enderlin *et al.*, 2009). Additionally, *IP-10* is a putative NCoR target gene with an activator protein 1 (AP1) site for the recruitment of c-Jun (Ghisletti *et al.*, 2009). We therefore chose this gene as a putative NCoR target gene and examined how NCoR modulates the invasion of cancer cells in a CK2-dependent manner. To confirm the selective involvement of NCoR and CK2 in the transcriptional regulation of *IP-10*, we assessed the level of another metastasis-related gene, *CXCL12*. Both knockdown of CK2 and NCoR commonly derepressed IP-10 transcription; however, the transcriptional level of CXCL12 was not altered, suggesting the

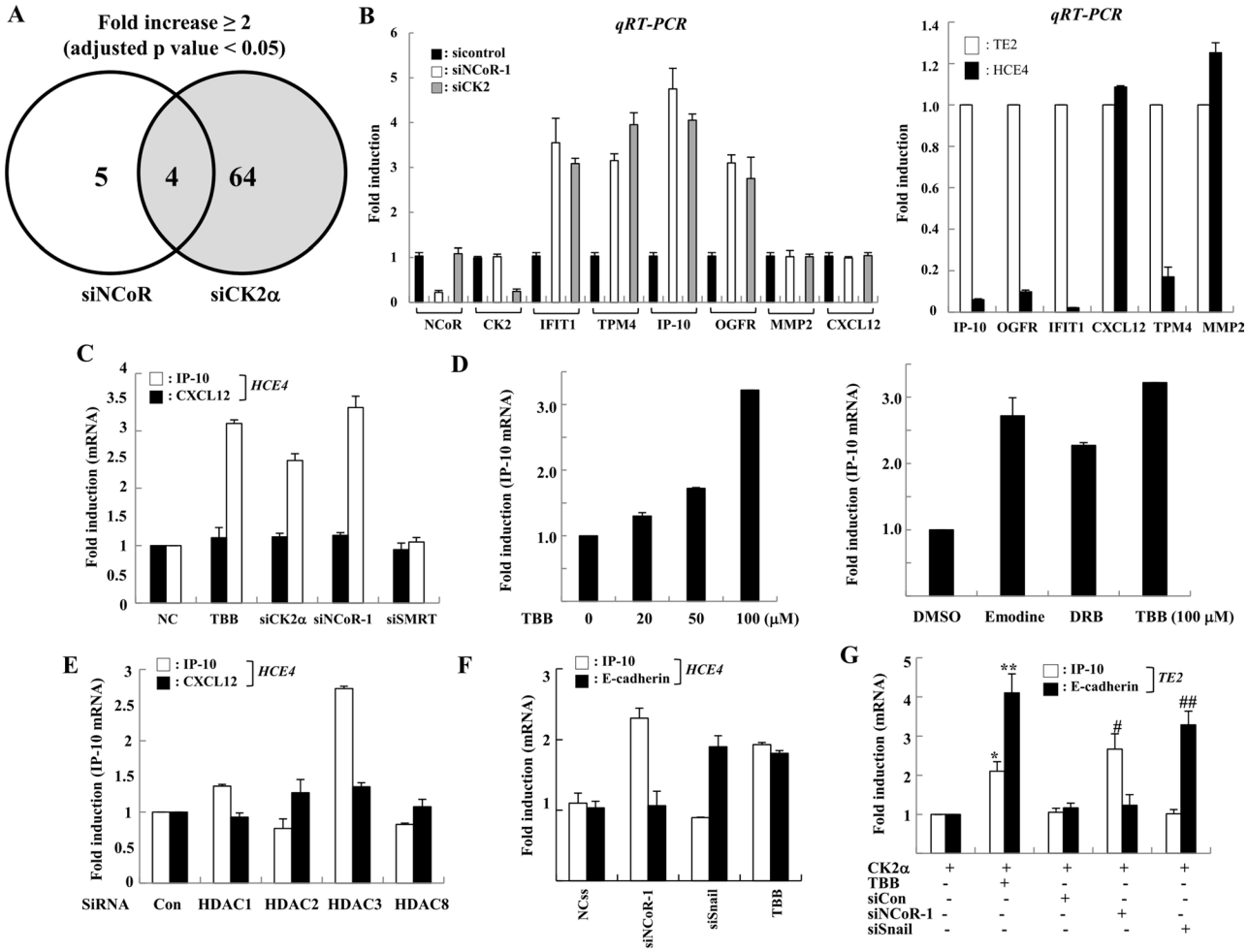

FIGURE 5: NCoR selectively represses transcription of the anti-tumorigenic gene *IP-10/CXCL10* in a CK2α-dependent manner. (A) HCE4 cells were transfected with siRNA against NCoR and CK2α, and the change in mRNA expression was analyzed by cDNA microarray analysis using the Illumina HumanRef-8 version 3 Expression BeadChip. Data outputs and the average intensity for each array were normalized against housekeeping genes located on each array. Differentially expressed genes were identified by comparison of the siCK2 sample set with the small-interfering control sample set, and the siNCoR-2 sample set with the small-interfering control sample set using $p < 0.05$ as the significance cutoff. Only fold changes greater than 2.0 were considered. (B) HCE4 cells were treated with siRNAs, and the levels of indicated genes were analyzed by real-time PCR (left). The relative levels of indicated genes between TE2 and HCE4 cells were analyzed by real-time PCR (right). All samples were normalized to human GAPDH. (C) HCE4 cells were treated with TBB (50 μM, 6 H) or indicated siRNAs, and the level of each gene was analyzed by real-time PCR. (D) HCE4 cells were treated with an increasing amount of indicated inhibitors, and then mRNAs were analyzed by real-time PCR. (E) HCE4 cells were treated with siRNAs against each HDAC, and the level of each gene was analyzed by real-time PCR. (F) HCE4 cells were treated with TBB (50 μM, 6 H) or indicated siRNAs, and the level of each gene was analyzed by real-time PCR. (G) TE2 cells were transfected with CK2α plasmid. After 24 h, cells were treated with indicated siRNAs or TBB (50 μm, 6 H), and the levels of the indicated genes were analyzed by real-time PCR. *, $p < 0.01$ vs. CK2α alone; **, $p < 0.05$ vs. CK2α alone; #, $p < 0.05$ vs. CK2α +.siCon; ##, $p < 0.05$ vs. CK2α + siCon.

selective regulation of IP-10 transcription by the CK2 and NCoR signaling network (Figure 5C). Notably, TBB inhibitors commonly derepressed IP-10 transcription (Figure 5D). Importantly, the knockdown of SMRT had no effect on the derepression of IP-10, emphasizing the unique role of NCoR in the transcriptional repression of IP-10 (Figure 5C). More importantly, knockdown of HDAC3, but not other class I HDACs, specifically relieved the transcriptional repression of IP-10 in a manner similar to siNCoR treatment, demonstrating the crucial role of the NCoR-HDAC3 axis in the transcriptional repression of IP-10 (Figure 5E). CK2 also promotes Snail1-mediated transcriptional repression of E-cadherin, which is critical for suppression of EMT (MacPherson *et al.*, 2010). Intriguingly, E-cadherin transcription was selectively derepressed by depletion of Snail1, but not by depletion of NCoR. Conversely, the derepression of IP-10 was observed only upon NCoR knockdown (Figures 5F and S9). Strikingly, CK2 failed to repress transcription of IP-10 and E-cadherin in the depletion of NCoR and Snail1, respectively, indicating that the CK2-mediated signaling network coordinately regulates the transcription of downstream target genes to promote oncogenesis by adapting to different sets of corepressor complexes (Figures 5G and S10).

Because NCoR corepressor complexes are known to mainly repress transcription via deacetylation of histone tails, we examined whether both NCoR and HDAC3 are recruited to the AP1-binding site of IP-10 via c-Jun to subsequently induce hypoacetylation of

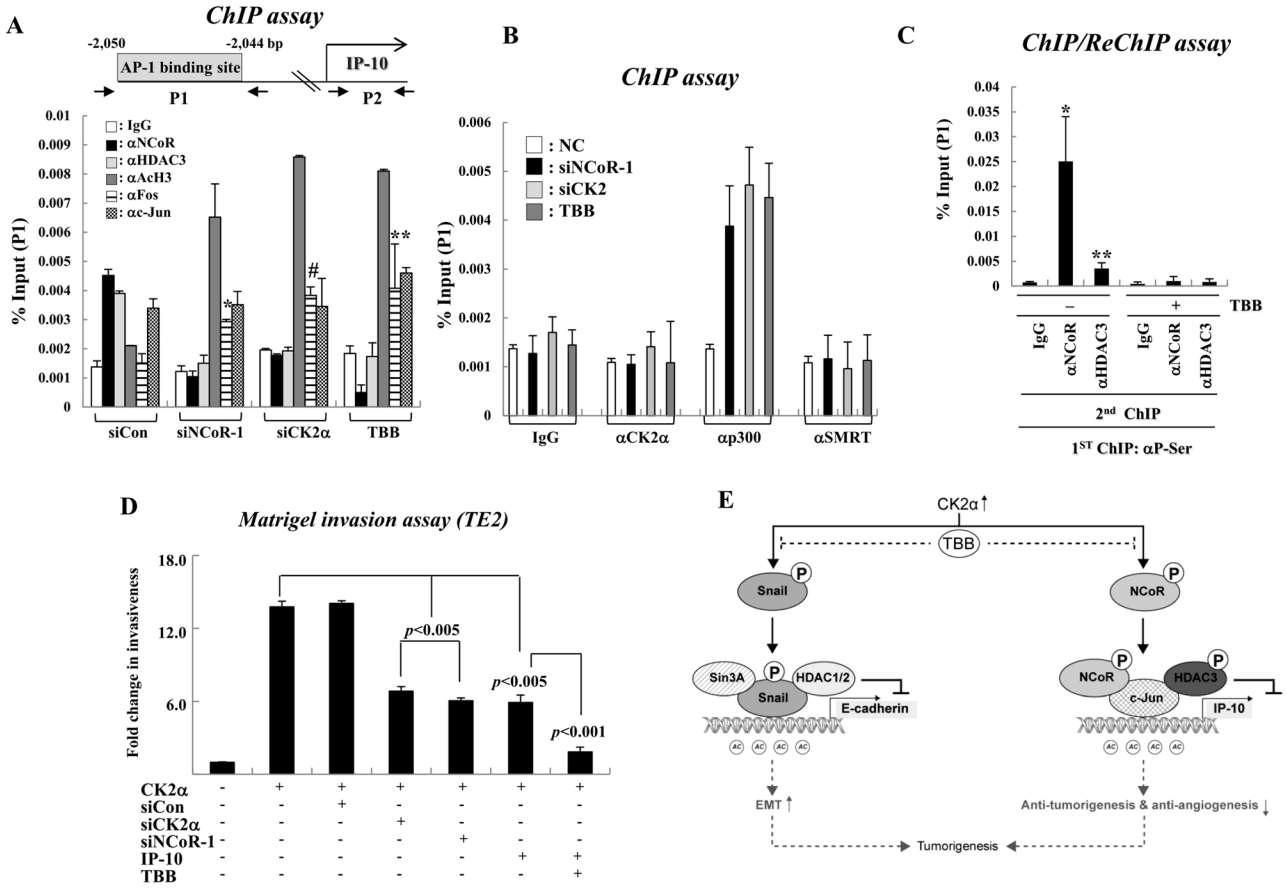

FIGURE 6: NCoR complexes repress IP-10 transcription at the epigenetic status via deacetylation of histone tails in a CK2α-dependent manner. (A and B) HCE4 cells were treated with TBB (50 μM, 6 H) or indicated siRNAs, and ChIP assays were performed with the indicated antibodies. The precipitated samples were analyzed by real-time PCR, and results are given as the percentage of input as means ± SD of three independent experiments. *, $p < 0.005$ vs. SiCon; #, $P < 0.01$ vs. SiCon; **, $p < 0.05$ vs. SiCon. (C) ChIP and reChIP assays were performed with the indicated antibodies. Error bars, SD ($n = 3$). *, $p < 0.05$ vs. IgG; **, $p < 0.01$ vs. IgG. (D) TE2 cells were transfected with indicated siRNAs and/or plasmids, and treated with TBB (50 μM, 6 H). The invading cells were counted in BioCoat Matrigel invasion chambers. (E) Model of our findings. In tumor cells with high CK2α activity, active CK2α phosphorylates NCoR and HDAC3 to repress IP-10 transcription, enhancing tumorigenesis. Additionally, CK2α phosphorylates Snail1 to repress E-cadherin transcription via an NCoR-independent pathway. Thus selective CK2α inhibition may be promising for anticancer therapy.

chromatin, ultimately leading to transcriptional repression. We first identified the AP1 site in human *IP-10*, because c-Jun is known to recruit NCoR to AP1 sites on NCoR target genes. A putative AP1 consensus sequence was identified at position −2050 (relative to the transcription start site) by sequence mining of *IP-10* (Figure 6A). Specific PCR primers were designed to amplify sequences (100–150 bp) surrounding the putative AP1-binding site (P1) and coding region (P2) of the *IP-10* gene (Figure 6A). Chromatin immunoprecipitation (ChIP) experiments showed the presence of c-Jun on the AP1-binding site of *IP-10*. Under the same experimental conditions, both NCoR and HDAC3 were also recruited to the AP1 site of *IP-10* in HCE4 cells, whereas reduced binding of HDAC3 was observed in siNCoR- and siCK2-treated HCE4 cells, presumably due to the decreased NCoR levels at the AP1 site (Figure 6A, P1). As controls, neither NCoR nor HDAC3 associated with the coding region of the *IP-10* gene (Figure S11A, P2). Consistent with previous studies, knockdown of c-Jun greatly abolished recruitment of the NCoR-HDAC3 complex to the AP1 site of *IP-10* (Figure S11B, P1). Importantly, the recruitment of CK2 to the AP1 site of *IP-10* was not observed regardless of TBB treatment, indicating the nonepigenetic role of CK2 in NCoR-mediated transcriptional repression of IP-10. Coincidently, TBB treatment resulted in an increase in histone acetylation and recruitment of the histone acetyltransferase p300, which corresponds with transcriptional activation of IP-10 (Figure 6B). More importantly, ChIP and reChIP experiments demonstrated that the phosphorylated form of NCoR was mainly bound to the AP1 site of the *IP-10* gene (Figure 6C). Because recruitment of Fos to the AP1 site was substantially increased in response to TBB treatment, we concluded that CK2 controls c-Jun-NCoR corepressor complex–mediated transcriptional repression of IP-10 by preventing recruitment of c-Jun-Fos coactivator complexes to *IP-10* (Figure 6B). Collectively these results show that NCoR complexes selectively repress IP-10 transcription at the epigenetic status via deacetylation of histone tails in a CK2-dependent manner.

Finally, the functional consequences of CK2-NCoR cascade–mediated transcriptional repression of IP-10 with respect to invasiveness of tumor cells were examined using a Matrigel invasion assay. CK2 overexpression consistently increased the invasion of TE2 cells; however, IP-10 restoration suppressed the CK2-induced invasion of

TE2 cells in a manner similar to NCoR and CK2 knockdown. The increased invasiveness of TE4 cells by CK2 seems to be NCoR-dependent, because the depletion of NCoR diminished the CK2-enhanced invasion of TE2 cells (Figure 6D). Further, the chorioallantoic membrane (CAM) assay again verified that the CK2-mediated invasion of HCE4 cells is dependent on NCoR by showing that siNCoR-treated HCE4 cells displayed complete loss of the tissue-invasive phenotype (Figure S12). These data collectively suggest that the CK2-NCoR cascade promotes invasiveness of tumor cells by transcriptional repression of IP-10.

DISCUSSION

Many studies have shown that elevated levels of CK2 are associated with tumorigenesis (Trembley *et al.*, 2009). High CK2 activity levels accelerated the formation and development of squamous cell cancer of the head and neck, lung squamous cell carcinoma, and metastatic breast and prostate cancer (Gapany *et al.*, 1995; Faust *et al.*, 2000; Babiker *et al.*, 2006; Giusiano *et al.*, 2010). Moreover, CK2-specific inhibitors significantly inhibited membrane invasion, adhesion, and migration of ovarian carcinoma cells. CK2 phosphorylates a broad spectrum of nuclear as well as cytoplasmic proteins in multiple aspects of gene expression (Ruzzene and Pinna, 2010). Importantly, a recent study has functionally implicated CK2 in E-cadherin down-regulation. Snail1 is known to be a transcriptional repressor of E-cadherin transcription and is also phosphorylated by CK2, leading to enhanced Snail1 stability and subsequent increase in E-cadherin transcriptional repression. For E-cadherin transcriptional repression, Snail1 has been shown to selectively interact with another corepressor complex, mSin3-HDAC1, but not with NCoR-SMRT (Peinado *et al.*, 2004). Our results demonstrate that CK2α phosphorylates NCoR to selectively repress transcription of the novel NCoR target gene *IP-10* and to enhance tumorigenesis without correlating with EMT and migration, because Snail1 knockdown had no effect on IP-10 expression. Moreover, NCoR knockdown had no effect on E-cadherin transcription. The exclusive roles of HDAC-containing corepressor complexes in transcriptional repression of a subset of target genes have been emphasized by several studies. For instance, previous studies regarding transcriptional repression of the thyroid hormone receptor (TR) target gene *deiodinase 1* (*D1*) have shown selective recruitment of unliganded TR-NCoR-HDAC3 complexes to the promoter region of *D1* (Yoon *et al.*, 2005). Furthermore, exclusive recruitment of sin3A-HDAC1-HDAC2 complexes to the endogenous E-cadherin promoter was shown, but not with other class I HDAC corepressor complexes, including HDAC3, indicating the unique role of corepressor complexes in the transcription repression of respective target genes (Peinado *et al.*, 2004).

Proto-oncoprotein c-Jun, which interacts with c-Fos protein to form a heterodimer, plays an important role in the transcriptional regulation, signal transduction, and tumorigenesis (Eferl and Wagner, 2003; Sancho *et al.*, 2009). c-Jun was recently shown to recruit NCoR to AP1 sites on NCoR-specific promoters to mediate anti-inflammatory signals (Ghisletti *et al.*, 2009). Our ChIP analysis also showed that c-Jun recruits NCoR-HDAC3 corepressor complexes to the AP1 site of IP-10 promoter along with the dissociation of c-Fos, leading to the histone hypoacetylation. Notably, TBB treatment induced the reassociation of c-Fos with c-Jun on the AP1 site of the *IP-10* gene along with the detachment of NCoR from c-Jun. These data are reminiscent of the c-Jun-Mbd3-NuRD repressor complex in the repression of intestinal stem cell marker Igr5 (Aguilera *et al.*, 2011). In that study, the assembly of c-Jun-Mbd3-NuRD repressor complex was relieved by JNK-mediated c-Jun N-terminal phosphorylation. Thus the exchange between corepressors and coactivators in c-Jun–mediated transcriptional regulation seems to be coordinately regulated by JNK-mediated phosphorylation. Interestingly, the component of NCoR corepressor complex, GPS2, was shown to inhibit the JNK-mediated c-Jun phosphorylation in an NCoR-dependent manner (Zhang *et al.*, 2002). Thus a plausible model would show GPS2 inhibiting the JNK-mediated phosphorylation of c-Jun to induce the binding of NCoR-HDAC3 corepressor complex to c-Jun, which would finally lead to the transcriptional repression of the *IP-10* gene. Future studies to investigate the role of GPS2 on the c-Jun-NCoR complex–mediated transcriptional repression of target genes will be interesting.

Analysis of the phosphorylation site in NCoR revealed that the CK2α phosphorylation motif of NCoR is identical to that of SMRT. Thus we initially expected an effect of CK2-dependent phosphorylation on the function of NCoR similar to that seen with SMRT. Interestingly, we found that silencing or inhibiting CK2α resulted in a reduced NCoR level, and MG132 treatment efficiently blocked the ubiquitin-dependent proteasomal degradation of NCoR. The effect of CK2α-dependent phosphorylation on protein stability was found to be unique to NCoR, because both CK2α knockdown and TBB treatment had no effect on SMRT levels. Notably, other kinase inhibitors failed to affect NCoR stability, indicating the unique role of CK2α in the regulation of NCoR stability. It is also noteworthy that the effect of TBB on NCoR stability seems to be greater than CK2 knockdown by siRNA. Because TBB is not absolutely unique to CK2α, we could not exclude the possibility of another regulatory mechanism for NCoR stability. Furthermore, the result from ChIP assays displayed the selective recruitment of NCoR, but not SMRT, to the AP1 site of IP-10. Thus, for the first time, we provide evidence for the differential effect of CK2-dependent phosphorylation on the function of SMRT and NCoR protein. In addition to regulating SMRT and NCoR function, CK2-mediated HDAC3 phosphorylation enhances histone deacetylase activity and nuclear translocation, leading to enhanced repressive function (Zhang *et al.*, 2005). Our results show that TBB treatment also blocks HDAC3 phosphorylation, as well as HDAC activity (unpublished data), leading to down-regulation of IP-10. Furthermore, silencing of HDAC3 also selectively derepresses IP-10 transcription in a manner similar to siNCoR or siCK2, suggesting the functional engagement of NCoR-HDAC3 corepressor complex in transcriptional repression of IP-10. These data collectively suggest that CK2 phosphorylates both NCoR and HDAC3, which enhances NCoR stability and HDAC3 activity and leads to increased potency and integrity of the NCoR-HDAC3 corepressor complex for IP-10 transcriptional repression.

IP-10 has recently been shown to inhibit growth, angiogenesis, and metastasis in experimental tumors (Keyser *et al.*, 2004; Tominaga *et al.*, 2007; Mei *et al.*, 2008). In addition, several clinical studies have demonstrated that the down-regulated IP-10 correlated with poor patient prognosis in human cancer (Sato *et al.*, 2007; Jiang *et al.*, 2010). Thus the suppression of IP-10 expression might result in drastic tumor growth and metastasis that accelerates tumor advancement. Intriguingly, as seen in our cDNA microarray data, IP-10 has been identified as a putative NCoR target gene containing an AP1 site for the recruitment of c-Jun (Ghisletti *et al.*, 2009). Thus we hypothesized that CK2 phosphorylates NCoR to promote the tumorigenic growth of cancer cells with IP-10 down-regulation. Diverse analysis of the invasion of HCE4 cells showed that NCoR modulates the invasiveness of cancer cells via transcriptional repression of IP-10 in a CK2-dependent manner. Consistently, overexpression of IP-10 had an opposite effect on the invasion of HCE4 cells. These

results confirmed the regulatory role of the CK2-NCoR cascade in the anti-tumorigenic effect of IP-10. Because IP-10 is known to be involved in antitumor immune responses via induction of cytotoxic T-lymphocyte migration to the tumor site (Huang *et al.*, 2002), we cannot exclude the possibility that CK2-NCoR cascade–mediated IP-10 down-regulation results in immune evasion of cancer cells, possibly leading to oncogenesis. Importantly, failure of the derepression of IP-10 by depletion of Snail1 again confirmed our notion that the CK2 signaling cascade likely promotes the invasion of tumor cells by suppressing a subset of genes with selective recruitment of corepressor complexes.

In summary, this study shows that CK2 promotes tumorigenesis via NCoR-dependent repression of the *IP-10* gene, which is independent of the Snail1-mediated EMT pathway. This work provides in vivo evidences that the CK2-NCoR signaling network selectively suppresses the transcription of IP-10 to promote invasion of human cancer cells. Thus this study highlights the importance of the novel CK2-NCoR signaling network in tumorigenesis (Figure 6D).

MATERIALS AND METHODS

Cell culture, plasmids, and antibodies

The human cervical epithelial adenocarcinoma cell line HeLa as well as two human esophageal cancer cell lines, TE2 and HCE4, were cultured in DMEM (Life Technologies, Gaithersburg, MD) supplemented with 10% (vol/vol) fetal bovine serum (FBS; Life Technologies), 100 U/ml penicillin (Life Technologies), and 0.1 mg/ml streptomycin (Life Technologies) at 37°C under 5% CO_2. MG132 was purchased from Calbiochem (Bad Soden, Germany), and a 10 mM stock was prepared in dimethyl sulfoxide (DMSO; Sigma-Aldrich, St. Louis, MO). The TE2-CK2 stable cell line that expresses CK2α was kindly provided by Kunhong Kim (Yonsei University, Seoul, Korea) and cultured in DMEM. The CK2 inhibitor TBB was prepared as a 50 mM stock solution in DMSO (Sigma-Aldrich). Control cultures received the same amounts of DMSO as experimental cultures, and final DMSO concentrations did not exceed 0.1%. Transient transfection was performed using Polyexpress (Excellgene, Gaithersburg, MD). Additionally, several kinase inhibitors, including $LiCl_2$ (GSK3β inhibitor; Amresco, Cleveland, OH), SP600125 (JNK1 inhibitor; Assay Designs, Ann Arbor, MI), SB-203580 (MEK-inhibitor; Assay Designs), wortmannin (PI3K inhibitor; Assay Designs), Akt inhibitor (Calbiochem), ERK inhibitor (Calbiochem), and H89 (PKA inhibitor; Assay Designs) were used to investigate the stabilization of NCoR1. The following antibodies were used: anti-CK2 (Upstate, Charlottesville, VA), anti-hemagglutinin (anti-HA; Sigma-Aldrich, and Covance, New York, NY), anti-FLAG (Sigma-Aldrich), anti–β-actin (Sigma-Aldrich), anti-GAPDH (Millipore, Bedford, MA), anti-NCoR (ATGEN, Seongnam, Gyeonggido, Korea), anti–E-cadherin, anti–MMP-9 (Calbiochem), anti-vimentin (Santa Cruz Biotechnology, Santa Cruz, CA), anti-p300 (Upstate), anti–c-Jun (Epitomics, Burlingame, CA), anti–acetyl-histone H3, anti-IP-10 (Santa Cruz Biotechnology), and anti-Myc (Cell Signaling, Danvers, MA). The antibody against phospho-Ser was from Zymed Laboratories (San Francisco, CA). The antibody against phospho-NCoR1 was raised against the synthetic peptide CQYETLpSDSDD by LabFrontier (Anyang, Gyeonggido, Korea). The antibodies against SMRT and HDAC3 were generated as described previously (Li *et al.*, 2000). Both CK2α and CK2β constructs were generated by PCR and cloned into the pSG5-KF2M1 and pSG5-KM2M1 (Sigma-Aldrich) plasmid vectors. The origins of pSG5-Flag-NCoR-1/2 (1–380), pSG5-Flag-NCoR-9/10 (714–1053), pSG5-Flag-NCoR-11/12 (1053–1476), pSG5-Flag-NCoR-13/14 (1487–1949), and pSG5-Flag-NCoR-15/16 (1985–2440) were described previously (Li *et al.*, 2000). Full-length pCMV-GFP-NCoR (1–2453) was previously described (Jonas and Privalsky, 2004). The FLAG-tagged Siah1 was obtained from DNASU Plasmid Repository (Arizona State University, Tempe, AZ).

Duolink in situ PLA analysis

Duolink in situ PLA analysis was performed according to the manufacturer's instructions (OLink Biosciences, Uppsala, Sweden). Briefly, paraformaldehyde-fixed cells were washed with phosphate-buffered saline, incubated for 15 min in 1.5% hydrogen peroxide, washed, and blocked with blocking solution. Primary rabbit antibody was applied, and the cells were incubated with PLUS and MINUS secondary PLA probes against rabbit immunoglobulin G (IgG) only or against both rabbit and mouse IgGs. The incubation was followed by hybridization and ligation, and then amplification was performed. After being mounted with Duolink mounting medium, samples were examined using an Olympus FluoView FV1000 confocal microscope (Olympus, Tokyo, Japan).

ChIP assays

ChIP assays were performed with the indicated antibodies as described previously (Yoon *et al.*, 2003b), but without SDS in all buffers. Eluted DNA was amplified with specific primers using SYBR Green PCR Master Mix (Applied Biosystems, Foster City, CA). Primers used in PCR were as follows: P1 (forward [F]: 5′-CCAGGCATTGTTTGAACTGC-3′; reverse [R]: 5′-AGCAAAAGATGTCTTGCACAAA-3′). P2 (F: 5′-GACTACCTCTCTCTAGAACT-3′; R: 5′-GATCTCAACACGTGGACAAA-3′). All reactions were normalized relative to input activities and are presented as means (± SD) of three independent experiments.

siRNA experiments

The siRNAs against NCoR1 or CK2α, as well as a nonspecific siRNA, were obtained from GenePharma (Shanghai, China). For siRNA transfection, HeLa and HCE4 cells were incubated with DMEM without FBS and antibiotics for 12 h, and transfected with 200 nM nonspecific siRNA, siRNA-NcoR1, and siRNA-CK2 using Lipofectamine 2000 following the manufacturer's protocol (Invitrogen, Carlsbad, CA). After 4 h, the medium was changed, and cells were incubated for 2 d. siRNAs against NCoR1 and CK2α were designed as follows: siNCoR-1 (F: 5′-GGUGAUAAUACCAAAGAAATT-3′; R: 5′-UUUCUUUGGUAUUAUCACCTT-3′), siNCoR-2 (F: 5′-GGUGAUAAUACCAAAGAAATT-3′; R: 5′-UUUCUUUGGUAUUAUCACCTT-3′), siNCoR-3 (F: 5′-GGCUCUCAAAGUUCAGACUTT-3′; R: 5′-AGTCTGAACTTTGAGAGCCTT-3′), siSMRT (F: 5′-GUUCAACACACUUGACAAATT-3′; R: 5′-UUUGUCAAGUGUGUUGGACTT-3′), siSnail1 (F: 5′-XTGCACATCCGAAGCCACAC-3′; R: 5′- GUGUGGCUUCGGAUGUGCATT-3′), siCK2 (F: 5′-CAGAAAGCUACGACUAAUATT-3′; R: 5′-RUAUUAGUCGUAGCUUUCUGTG-3′), and sic-Jun (F: 5′-GAGCGGACCUUAUGGCUACUU-3′; R: 5′- GUAGCCAUAAGGUCCGCUCUU-3′). The siRNA sequences against HDAC1, HDAC2, HDAC3, and HDAC8 were previously described (Kim *et al.*, 2010).

Real-time PCR analysis

Real-time PCR analysis and quantification were performed with SYBR Green PCR Master Mix reagents on an ABI Prism 7300 Sequence Detection System. The singularity and specificity of amplification were verified using 7300 System Software (ABI). All samples were normalized to human GAPDH. Primer sequences for amplification of IP-10 RNA were 5′-CTGCCATTCTGATTTGCTGC-3′ (F) and 5′-GATGGCCTTCGATTCTGGAT-3′ (R). Primer sequences for amplification of E-cadherin RNA were 5′-AACGCATTGCCACATACACT-3′ (F) and

5′-CCATGACAGACCCCTTAAAGA-3′ (R). Primer sequences for amplification of CXCL12 RNA were 5′-GGTCGTGCTGGTCCTCGT-3′ (F) and 5′-TTAGCTTCGGGTCAATGCAC-3′ (R). Primer sequences for amplification of DIO2 RNA were 5′-GCAGCTTCTGGAGCGTTTCT-3′ (F) and 5′-TGTCTCTGCACAATGCACACA-3′ (R). Primer sequences for amplification of IFIT1 RNA were 5′-ACTGGCAGAAGCCCAGACTT-3′ (F) and 5′-GCCCGTTCATAATTCTTTCCT-3′ (R). Primer sequences for amplification of TPM4 RNA were 5′-GGACAGGGCTCAGGAACGA-3′ (F) and 5′-TTGAGCTGCATCTCCTGAATCT-3′ (R). All reactions were performed in triplicate. Relative expression levels and SDs were calculated using the comparative method.

cDNA microarray analysis

HCE4 cells were transfected with 100 pmol of control siRNA, siCK2, or siNCoR. Biotinylated cRNA was obtained using a total RNA amplification kit (Ambion, Austin, TX) according to the manufacturer's instructions. Briefly, 550 ng of total RNA was reverse-transcribed to cDNA using a T7 oligo (dT) primer. Second-strand cDNA was synthesized, in vitro transcribed, and labeled with biotin-NTP. After purification, the cRNA was quantified using the ND-1000 Spectrophotometer (NanoDrop, Wilmington, DE). Labeled cRNA samples (750 ng) were hybridized to human-8 expression bead arrays for 16–18 h at 58°C, according to the manufacturer's instructions (Illumina, San Diego, CA). Detection of the array signal was performed using Amersham fluorolink streptavidin-Cy3 (GE Healthcare Life Sciences, Little Chalfont, UK) according to the bead array manual. Arrays were scanned with an Illumina bead array reader confocal scanner according to the manufacturer's instructions. Array data export processing and analysis were performed using Illumina GenomeStudio version 2009.2 (Gene Expression Module v1.5.4). Data outputs and the average intensity for each array from two independent experiments were normalized against housekeeping genes located on each array. Differentially expressed genes were identified by comparison of the siCK2 sample set with the small-interfering control sample set, and the siNCoR sample set to the small-interfering control sample set, using $p < 0.05$ as the significance cutoff. Only fold changes greater than 2.0 were considered.

In vitro kinase assay

GST-fusion proteins were incubated with 500 U of recombinant CK2α (ATGEN) in the presence of kinase reaction buffer (10 µl 5× kinase buffer, 10 µl magnesium/ATP cocktail solution 90 µl 75 mM $MgCl_2$/500 mM ATP plus 10 µl [100 µCi] of [γ-^{32}P]ATP [3000 Ci/mmol]) in a total volume of 50 µl for 30 min at 30°C. Reactions were terminated by washing twice with 1× kinase buffer. Samples were resuspended in 15 µl 5× SDS sample loading buffer and boiled for 5 min. After electrophoresis, SDS polyacrylamide gels were stained with Coomassie blue and dried, and the phosphorylated products were visualized by autoradiography or quantified by phosphorimager analysis.

Matrigel invasion assays

In vitro cell invasiveness was determined by the ability of cells to transmigrate through a layer of extracellular matrix in BioCoat Matrigel invasion chambers (SPL Lifescience, Pocheon, Gyeonggido, Korea). Posttransfected cells (48 h) were trypsinized and seeded at a density of 2.0×10^4 per insert. After 24 h, noninvading cells were removed with cotton swabs. Invading cells were fixed with 100% methanol and stained with 1% crystal violet (Sigma-Aldrich) before enumeration under an inverted microscope. Data are expressed as the mean ± SD of at least three independent experiments.

Chick CAM invasion assay

HCE4 cells were labeled with Fluoresbrite carboxylate nanospheres (Polysciences, Warrington, PA) and cultured on CAMs of 11-d-old chick embryos for 3 d. Invasion was monitored in cross-sections of the fixed CAMs by fluorescence microscopy.

Statistical analysis

Statistical analyses were done using Student's *t* test with Bonferroni for multiple comparisons. $p < 0.05$ was considered significant.

ACKNOWLEDGMENTS

We thank D. S. Jang for his excellent support with medical illustration. This study was supported by a National Research Foundation of Korea grant (no. 2011-0030709) funded by the Korean government.

REFERENCES

Aguilera C, Nakagawa K, Sancho R, Chakraborty A, Hendrich B, Behrens A (2011). c-Jun N-terminal phosphorylation antagonises recruitment of the Mbd3/NuRD repressor complex. Nature 469, 231–235.

Babiker AA, Ronquist G, Nilsson B, Ekdahl KN (2006). Overexpression of ecto-protein kinases in prostasomes of metastatic cell origin. Prostate 66, 675–686.

Chen YY, Chiang SY, Lin JG, Ma YS, Liao CL, Weng SW, Lai TY, Chung JG (2010). Emodin, aloe-emodin and rhein inhibit migration and invasion in human tongue cancer SCC-4 cells through the inhibition of gene expression of matrix metalloproteinase-9. Int J Oncol 36, 1113–1120.

Christensen B, Nielsen MS, Haselmann KF, Petersen TE, Sorensen ES (2005). Post-translationally modified residues of native human osteopontin are located in clusters: identification of 36 phosphorylation and five O-glycosylation sites and their biological implications. Biochem J 390, 285–292.

Eferl R, Wagner EF (2003). AP-1: a double-edged sword in tumorigenesis. Nat Rev Cancer 3, 859–868.

Enderlin M *et al.* (2009). TNF-α and the IFN-γ-inducible protein 10 (IP-10/CXCL-10) delivered by parvoviral vectors act in synergy to induce antitumor effects in mouse glioblastoma. Cancer Gene Ther 16, 149–160.

Faust RA, Tawfic S, Davis AT, Bubash LA, Ahmed K (2000). Antisense oligonucleotides against protein kinase CK2-α inhibit growth of squamous cell carcinoma of the head and neck in vitro. Head Neck 22, 341–346.

Gapany M, Faust RA, Tawfic S, Davis A, Adams GL, Ahmed K (1995). Association of elevated protein kinase CK2 activity with aggressive behavior of squamous cell carcinoma of the head and neck. Mol Med 1, 659–666.

Ghisletti S, Huang W, Jepsen K, Benner C, Hardiman G, Rosenfeld MG, Glass CK (2009). Cooperative NCoR/SMRT interactions establish a corepressor-based strategy for integration of inflammatory and anti-inflammatory signaling pathways. Genes Dev 23, 681–693.

Giusiano S *et al.* (2010). Protein kinase CK2α subunit over-expression correlates with metastatic risk in breast carcinomas: Quantitative immunohistochemistry in tissue microarrays. Eur J Cancer 47, 792–801.

Guo C, Yu S, Davis AT, Wang H, Green JE, Ahmed K (2001). A potential role of nuclear matrix-associated protein kinase CK2 in protection against drug-induced apoptosis in cancer cells. J Biol Chem 276, 5992–5999.

Hoberg JE, Yeung F, Mayo MW (2004). SMRT derepression by the IκB kinase α: a prerequisite to NF-κB transcription and survival. Mol Cell 16, 245–255.

Huang H, Liu Y, Xiang J (2002). Synergistic effect of adoptive T-cell therapy and intratumoral interferon γ-inducible protein-10 transgene expression in treatment of established tumors. Cell Immunol 217, 12–22.

Jiang Z, Xu Y, Cai S (2010). CXCL10 expression and prognostic significance in stage II and III colorectal cancer. Mol Biol Rep 37, 3029–3036.

Jonas BA, Privalsky ML (2004). SMRT and N-CoR corepressors are regulated by distinct kinase signaling pathways. J Biol Chem 279, 54676–54686.

Keyser J, Schultz J, Ladell K, Elzaouk L, Heinzerling L, Pavlovic J, Moelling K (2004). IP-10-encoding plasmid DNA therapy exhibits anti-tumor and anti-metastatic efficiency. Exp Dermatol 13, 380–390.

Kim HC, *et al.* (2010). HDAC3 selectively represses CREB3-mediated transcription and migration of metastatic breast cancer cells. Cell Mol Life Sci 67, 3499–3510.

Landesman-Bollag E, Song DH, Romieu-Mourez R, Sussman DJ, Cardiff RD, Sonenshein GE, Seldin DC (2001). Protein kinase CK2: signaling and tumorigenesis in the mammary gland. Mol Cell Biochem 227, 153–165.

Li J, Wang J, Nawaz Z, Liu JM, Qin J, Wong J (2000). Both corepressor proteins SMRT and N-CoR exist in large protein complexes containing HDAC3. EMBO J 19, 4342–4350.

MacPherson MR, Molina P, Souchelnytskyi S, Wernstedt C, Martin-Perez J, Portillo F, Cano A (2010). Phosphorylation of serine 11 and serine 92 as new positive regulators of human Snail1 function: potential involvement of casein kinase-2 and the cAMP-activated kinase protein kinase A. Mol Biol Cell 21, 244–253.

Mei K, Wang L, Tian L, Yu J, Zhang Z, Wei Y (2008). Antitumor efficacy of combination of interferon-gamma-inducible protein 10 gene with gemcitabine, a study in murine model. J Exp Clin Cancer Res 27, 63.

Peinado H, Ballestar E, Esteller M, Cano A (2004). Snail mediates E-cadherin repression by the recruitment of the Sin3A/histone deacetylase 1 (HDAC1)/HDAC2 complex. Mol Cell Biol 24, 306–319.

Perissi V, Aggarwal A, Glass CK, Rose DW, Rosenfeld MG (2004). A corepressor/coactivator exchange complex required for transcriptional activation by nuclear receptors and other regulated transcription factors. Cell 116, 511–526.

Perissi V, Jepsen K, Glass CK, Rosenfeld MG (2010). Deconstructing repression: evolving models of co-repressor action. Nat Rev Genet 11, 109–123.

Ruzzene M, Pinna LA (2010). Addiction to protein kinase CK2: a common denominator of diverse cancer cells?. Biochim Biophys Acta 1804, 499–504.

Sancho R, Nateri AS, de Vinuesa AG, Aguilera C, Nye E, Spencer-Dene B, Behrens A (2009). JNK signalling modulates intestinal homeostasis and tumourigenesis in mice. EMBO J 28, 1843–1854.

Sato E, Fujimoto J, Toyoki H, Sakaguchi H, Alam SM, Jahan I, Tamaya T (2007). Expression of IP-10 related to angiogenesis in uterine cervical cancers. Br J Cancer 96, 1735–1739.

Seol W, Mahon MJ, Lee YK, Moore DD (1996). Two receptor interacting domains in the nuclear hormone receptor corepressor RIP13/N-CoR. Mol Endocrinol 10, 1646–1655.

Shin S, Lee Y, Kim W, Ko H, Choi H, Kim K (2005). Caspase-2 primes cancer cells for TRAIL-mediated apoptosis by processing procaspase-8. EMBO J 24, 3532–3542.

Soderberg O *et al*. (2006). Direct observation of individual endogenous protein complexes in situ by proximity ligation. Nat Methods 3, 995–1000.

Song DH, Dominguez I, Mizuno J, Kaut M, Mohr SC, Seldin DC (2003). CK2 phosphorylation of the armadillo repeat region of β-catenin potentiates Wnt signaling. J Biol Chem 278, 24018–24025.

Tiefenbach J, Novac N, Ducasse M, Eck M, Melchior F, Heinzel T (2006). SUMOylation of the corepressor N-CoR modulates its capacity to repress transcription. Mol Biol Cell 17, 1643–1651.

Tominaga M, Iwashita Y, Ohta M, Shibata K, Ishio T, Ohmori N, Goto T, Sato S, Kitano S (2007). Antitumor effects of the MIG and IP-10 genes transferred with poly [d,l-2,4-diaminobutyric acid] on murine neuroblastoma. Cancer Gene Ther 14, 696–705.

Trembley JH, Wang G, Unger G, Slaton J, Ahmed K (2009). Protein kinase CK2 in health and disease: CK2: a key player in cancer biology. Cell Mol Life Sci 66, 1858–1867.

Yoon HG, Chan DW, Huang ZQ, Li J, Fondell JD, Qin J, Wong J (2003a). Purification and functional characterization of the human N-CoR complex: the roles of HDAC3, TBL1 and TBLR1. EMBO J 22, 1336–1346.

Yoon HG, Chan DW, Reynolds AB, Qin J, Wong J (2003b). N-CoR mediates DNA methylation-dependent repression through a methyl CpG binding protein Kaiso. Mol Cell 12, 723–734.

Yoon HG, Choi Y, Cole PA, Wong J (2005). Reading and function of a histone code involved in targeting corepressor complexes for repression. Mol Cell Biol 25, 324–335.

Zhang J, Kalkum M, Chait BT, Roeder RG (2002). The N-CoR-HDAC3 nuclear receptor corepressor complex inhibits the JNK pathway through the integral subunit GPS2. Mol Cell 9, 611–623.

Zhang X, Ozawa Y, Lee H, Wen YD, Tan TH, Wadzinski BE, Seto E (2005). Histone deacetylase 3 (HDAC3) activity is regulated by interaction with protein serine/threonine phosphatase 4. Genes Dev 19, 827–839.

Zhou Y, Gross W, Hong SH, Privalsky ML (2001). The SMRT corepressor is a target of phosphorylation by protein kinase CK2 (casein kinase II). Mol Cell Biochem 220, 1–13.